Title: Radiative Corrections to the Neutrino Counting Process e+e−→νν̄γ

Author: Karol Kołodziej, Jan Polak, Marek Zrałek

Citation style: Kołodziej Karol, Polak Jan, Zrałek Marek. (1989). Radiative Corrections to the Neutrino Counting Process e+e−→νν̄γ. "Acta Physica Polonica. B" (1989, no. 7, s. 591-601).

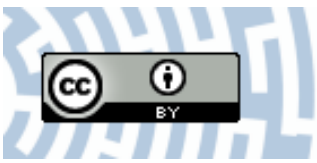

RADIATIVE CORRECTIONS TO THE NEUTRINO COUNTING PROCESS $e^+e^- \to \bar{\nu}\nu\gamma$*

By K. Kołodziej, J. Polak and M. Zrałek

Department of Theoretical Physics, Silesian University, Katowice**

(Received November 24, 1988)

The standard model weak corrections to the process $e^+e^- \to \bar{\nu}\nu\gamma$ which are important from the point of view of consistent renormalization are calculated. The calculations of the hard bremsstrahlung corrections to the process are done and they are found to be in good agreement with the former results.

PACS numbers: 12.10.Dm

1. Introduction

The reaction $e^+e^- \to \bar{\nu}\nu\gamma$ has been proposed as one which can provide information about the number of light neutrino species [1, 2, 3]. Its main advantage over other methods is that the cross section of $e^+e^- \to \bar{\nu}\nu\gamma$ would increase by $\sim 33\%$ if there existed the light neutrino of the fourth generation. Thus, to draw the information, it is enough to compare theoretical predictions with the data from neutrino counting experiments planned at LEP and SLC. However, to make this comparison properly one has not only to calculate the Born cross section, but also to calculate radiative corrections as well as to estimate a background to the process.

Virtual one loop QED and soft photon corrections to $e^+e^- \to \bar{\nu}\nu\gamma$ were calculated in [4, 5] and the result was confirmed in [6]. The corrections have been found to diminish the Born cross section by $\sim 50\%$. Thel virtual and soft corrections interfere with the correction coming from hard bremsstrahlung process $e^+e^- \to \bar{\nu}\nu\gamma\gamma$ where one photon is lost and the resulting corrections diminish the Born cross section by several per cent.

The main background to the reaction $e^+e^- \to \bar{\nu}\nu\gamma$ comes from the radiative Bhabha scattering $e^+e^- \to e^+e^-\gamma$ and it was studied in [7]. Radiative corrections to the background process were investigated in [8] and they were found to be small. Other sources of the background were discussed in [3].

* Work supported in part by the program CPBP 01.03.

** Address: Instytut Fizyki Teoretycznej, Uniwersytet Śląski, Uniwersytecka 4, 40-007 Katowice, Poland.

Considering only the photonic corrections to $e^+e^- \to \bar{\nu}\nu\gamma$ it is not possible to renormalize one loop eeZ Green function within the OS scheme of the QED. In order to renormalize the axial vector part of the vertex an additional renormalization constant has to be introduced. In Refs [4, 5] it was assumed that the counterterms to the vector and axial vector parts of the eeZ coupling are the same as the counterterm to the eeγ vertex. Such a pseudo-QED treatment may lead to the result different from the GSW treatment.

In the present work we have included a set of weak corrections to the process $e^+e^- \to \bar{\nu}\nu\gamma$ which allows to perform a consistent renormalization within the OS scheme of the Glashow-Salam-Weinberg (GSW) model as well as gives the idea about the size of the weak corrections to the neutrino counting process. Moreover, we have repeated the calculation of hard bremsstrahlung corrections and have obtained numerical results for radiatively corrected photon energy distribution for specific, but realistic experimental set-up.

2. *One loop weak corrections*

As it has been shown in Ref. [3], the reaction

$$e^-(p_1)+e^+(p_2) \to \nu(q_1)+\bar{\nu}(q_2)+\gamma(k) \tag{1}$$

for energies a few GeV above the Z production threshold is dominated by the annihilation channel which results in the fact that the cross section is almost proportional to the number of light neutrino species. This is what makes reaction (1) so useful for counting the neutrinos. Feynman diagrams that contribute to the reaction (1) in the first order are depicted in Fig. 1.

Since the contribution of the t-channel W boson and Z–W interference is very small, in order to find virtual corrections to (1) it is enough to consider loop diagrams obtained by attaching virtual gauge bosons lines, where possible, to the tree level diagrams with the Z boson exchange of Fig. 1a and b. Photonic one loop diagrams taken into account in [4, 5] are shown in Fig. 2. In order to estimate weak corrections to the process (1) as well

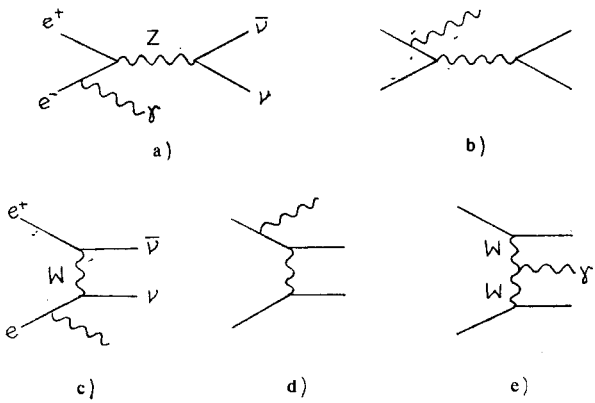

Fig. 1. Feynman diagram of the process $e^+e^- \to \bar{\nu}\nu\gamma$ in the first order

as to apply the on-mass-shell renormalization scheme (OS) [9] of the GSW model, in the present work we include weak corrections to the vertices eeZ, $\nu\nu Z$, and $\nu\nu\gamma$, represented by the diagrams of Fig. 3a, b, and c, respectively, together with electroweakly corrected Z propagator and $Z\gamma$ mixing.

Vertex Green functions corresponding to the diagrams of Fig. 3a, b, and c have the following form

$$\Gamma^{\mu}_{eeZ}(p_1-k,\,-p_2) = (A+C\gamma_5)\gamma^{\mu}+[(B_1+D_1\gamma_5)(p_1-k)^{\mu}$$

$$+(B_2+D_2\gamma_5)(-p_2)^{\mu}](\hat{p}_1-\hat{k}), \tag{2a}$$

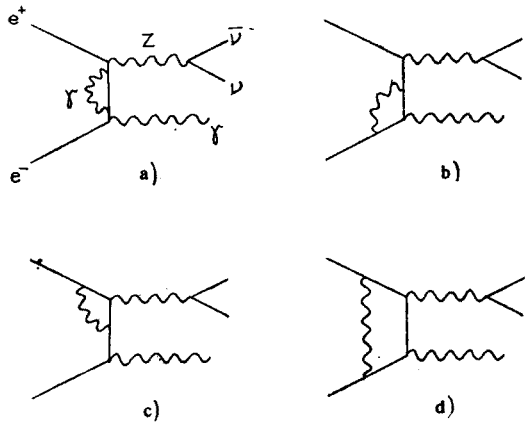

Fig. 2. One loop photonic Feynman diagrams obtained from the diagram of Fig. 1a

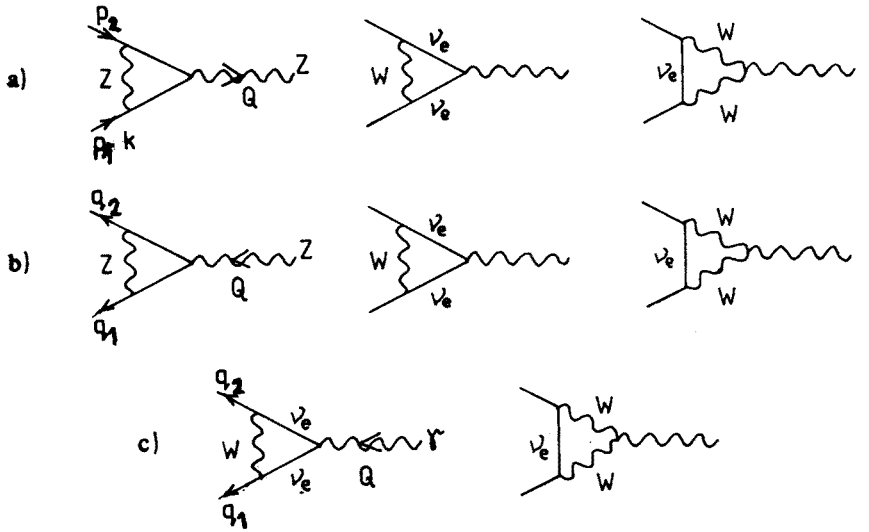

Fig. 3. One loop weak vertex corrections of the process $e^+e^- \to \bar{\nu}\nu\gamma$ considered in the paper

where we have used the on-shell condition for the momenta $\hat{p}_1$ and $\hat{p}_2$,

$$\Gamma^{\mu}_{\nu\nu Z}(-q_1, q_2) = F\gamma^{\mu}(1-\gamma_5), \tag{2b}$$

$$\Gamma^{\mu}_{\nu\nu\gamma}(-q_1, q_2) = G\gamma^{\mu}(1-\gamma_5), \tag{2c}$$

where we have used the on-shell condition for the momenta $\hat{q}_1$ and $\hat{q}_2$.

The three point Feynman amplitudes which are necessary to obtain the Green functions (2) are written down in [9]. They contain integrals over Feynman parameters. The integrals with higher powers of the parameters in the nominator are reduced to the integrals with the first power of one parameter and the zero power of the other following the method of Passarino and Veltman [10]. The reduction is performed by means of the program for algebraic manipulations REDUCE [11]. Next we calculate the resulting integrals either using the general formula of 't Hooft and Veltman [12] or, which is easier in the case of the $\nu\nu Z$ and $\nu\nu\gamma$ vertices, performing simple integration from the very beginning. During the calculations we neglect the electron mass where it is possible. We do not present the analytical formulae for the formfactors because they are too lengthy.

The one loop virtual and soft photon corrected cross section reads

$$\frac{d^2\sigma^{\nu+s}}{dxdy} = \frac{d^2\sigma_0^Z}{dxdy}\left\{1+\delta_{QED}^{\nu+s}+\left(\frac{\tau}{\kappa}+\frac{\kappa}{\tau}+\frac{2sQ^2}{\tau\kappa}\right)^{-1}[\delta_w(\kappa,\tau)+\delta_w(\tau,\kappa)]\right\}+\frac{d^2\sigma_0^{T-Z}}{dxdy}, \tag{3}$$

where $s = (p_1+p_2)^2$, $x = 2k/\sqrt{s}$ is the photon energy in units of beam energy, $y = \cos\theta$, with θ being the angle between $\vec{k}$ and $\vec{p}_1$, κ and τ are Brown–Feynman variables defined by

$$\kappa = 2p_1\cdot k = \frac{sx}{2}(1-\beta y),$$

$$\tau = 2p_2\cdot k = \frac{sx}{2}(1+\beta y),$$

with $\beta = (1-4m_e^2/s)^{1/2} \approx 1-2m_e^2/s$, and $Q^2 = s(1-x)$ is the Z momentum squared. $d^2\sigma_0^Z/dxdy$ is the cross section coming from the diagrams of Fig. 1a, b and it is given by

$$\frac{d^2\sigma_0^Z}{dxdy} = \frac{N_\nu\alpha^3}{3}\,\frac{M_Z^4[1+(1-4\sin^2\theta_w)]Q^2x}{2^7A^2s}\,|Z(Q^2)|^2\left(\frac{\tau}{\kappa}+\frac{\kappa}{\tau}+\frac{2sQ^2}{\tau\kappa}\right)^{-1}, \tag{4}$$

where N_ν denotes the number of light neutrino generations, $A = \dfrac{\pi\alpha}{\sqrt{2}G_\mu}$ with G_μ being the Fermi constant calculated from muon decay, $Z(Q^2)$ is electroweakly corrected Z propagator

$$Z(Q^2) = [Q^2-M_Z^2-\Sigma_Z(Q^2)]^{-1}, \tag{5}$$

with $\Sigma_Z(Q^2)$ being the one loop Z self energy. $d^2\sigma_0^{T-Z}/dxdy$ stands for terms coming from the square of the diagrams of Fig. 1c, d, e and their interference with the diagrams of Fig. 1a, b. These terms are written down in Ref. [4] $\delta_{QED}^{\nu+s}$ represents virtual and soft photonic

corrections and it can be found in Refs [4, 5]. The weak correction δ_W can be expressed in terms of the formfactors of formulae (2) as follows

$$\delta_W(\kappa,\tau) = 2\left(\frac{\tau}{\kappa}+\frac{sQ^2}{\tau\kappa}\right)\mathrm{Re}\left\{\frac{1}{A_0^2+C_0^2}\left[A_0A(\kappa,\tau)+C_0C(\kappa,\tau)\right.\right.$$
$$-\frac{s}{2}\left(\frac{\tau}{\kappa}+\frac{sQ^2}{\tau\kappa}\right)^{-1}(A_0B(\kappa,\tau)+C_0D(\kappa,\tau))$$
$$\left.\left.+\frac{A_0}{F_0}\frac{G(Q^2)}{Q^2Z(Q^2)}-\frac{A_0}{Q^2}\Sigma_{\gamma Z}(Q^2)\right]+\frac{F(Q^2)}{F_0}\right\}, \qquad (6)$$

where $A_0 = -\dfrac{1-4\sin^2\theta_W}{2\sin 2\theta_W}$ and $C_0 = -\dfrac{1}{2\sin 2\theta_W}$ are the tree level vector and axial vector couplings of the Z to electrons, $F_0 = -C_0$ is the tree coupling of the Z to neutrinos, $B = B_1+B_2$ and $D = D_1+D_2$. The analytical expresions for the formfactors involved in (6) are written down in Ref. [13]. The electroweakly one-loop corrected Z self energy $\Sigma_Z(Q^2)$ and Zγ mixing $\Sigma_{\gamma Z}(Q^2)$ can be found in [9] (formulae (5.7) and (5.14), respectively).

Formula (6) does not include all the electroweak corrections to the process $e^+e^- \to \bar{\nu}\nu\gamma$ for energies in the vicinity of the Z production threshold. The collection of Feynman diagrams for the whole set of electroweak corrections is shown in Fig. 4. From the comparison

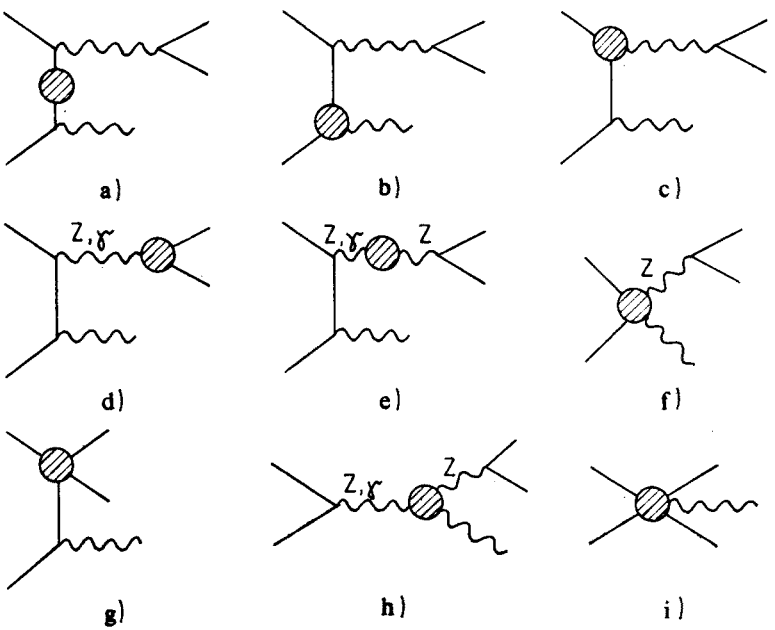

Fig. 4. One loop Feynman diagrams obtained from the diagram of Fig. 1a corresponding to the whole set of electroweak corrections

of Figs 2–4 it is seen that we have not considered weak corrections to the eeγ vertex (Fig. 4b) and to the electron self energy (Fig. 4a). This seems to be justified because the momentum transfer for them is much below the weak gauge bosons resonance energy. The contribution of anomaly diagrams (Fig. 4h) are of $O(m_t/\sqrt{s})$. For the t quark it is suppressed by three heavy propagators of the t. We also do not include weak corrections coming from box diagrams. Most of them contain at least two heavy gauge bosons propagators, but the most important one, similar to the QED box of Fig. 2d with the photonic propagator substituted by the Z propagator, is not taken into account for technical reasons only.

Although we do not consider all of the weak corrections we are able to perform a consistent renormalization and to give the idea about the range of the weak corrections to the process $e^+e^- \to \bar{\nu}\nu\gamma$. The effect of the weak corrections considered is of a few per cent range.

3. *Hard bremsstrahlung corrections*

Since the process

$$e^-(p_1)+e^+(p_2) \to \nu(q_1)+\bar{\nu}(q_2)+\gamma(k_1)+\gamma(k_2), \tag{7}$$

where both photons are hard, may imitate the $e^+e^- \to \bar{\nu}\nu\gamma$ reaction when one of the photons is lost, we have to estimate the contribution of it to the main process. There are six Feynman diagrams which contribute to (7) (see Fig. 5). We calculate the matrix element squared for reaction (7) by means of traditional trace technique with the use of REDUCE. We neglect the electron mass everywhere except for the case when one of the photons is collinear to the initial beam.

The unpolarized cross section integrated over a phase space of the neutrinos reads

$$\frac{d\sigma}{dx_1} = \frac{N_\nu}{3} \frac{\alpha^4 M_Z^4[1+(1-4\sin^2\theta_W)^2]}{2^{15}\pi^2 A^2} |Z(Q^2)|^2$$

$$\times \frac{s x_1 x_2^2 Q^2}{s(1-x_1)-Q^2} \left(-g_{\mu\nu}+\frac{Q_\mu Q_\nu}{Q^2}\right) m^{\mu\nu} dQ^2 dy_1 dy_2 d\varphi, \tag{8}$$

where $x_i = \dfrac{2k_i}{\sqrt{s}}$ and $y_i = \cos\theta_i$ $(i = 1, 2)$ are photon energies in units of beam energy and cosines of photon angles with respect to the incident beam in the e^+e^- CM system, φ is the azimuthal angle of one photon related to the plane determined by the beam line and the momentum of the other photon. Now $Q^2 = (p_1+p_2-k_1-k_2)^2$ and $Z(Q^2)$ is given by (5). The $m^{\mu\nu}$ includes traces along the electron lines together with the electron propagators and it can be found in the Appendix. Because of the collinear electron mass singularity and the resonant character of the Z boson, the cross section (8) is very peaked. In order to integrate it, we apply the standard Monte Carlo integration procedure RIWIAD [14], but in order to obtain a good accuracy we generate random numbers according to the

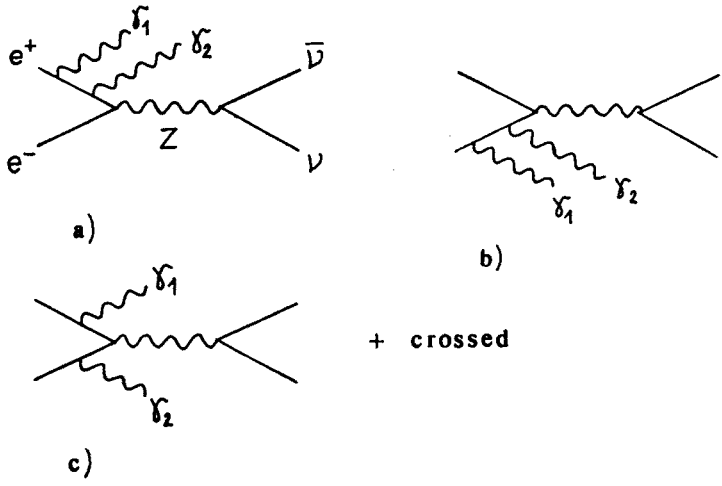

Fig. 5. Feynman diagrams of the process $e^+e^- \to \bar{\nu}\nu\gamma\gamma$

approximated distribution

$$\frac{d\sigma_{\text{app}}}{dx_1} \sim |Z(Q^2)|^2 dQ^2 \frac{dy_1}{1-\beta^2 y_1^2} \frac{dy_2}{1-\beta^2 y_2^2} d\varphi, \tag{9}$$

where $\beta = (1-4m_e^2/s)^{1/2} \approx 1-2m_e^2/s$. We have omitted the factor on the right hand side of (9) because the approximated distribution has to be normalized to unity. Distribution (9) can be easily integrated analytically and the resulting equations for the random variables satisfying (9) can be also solved analytically, which allows to save computational time.

There are three phase space regions in which the final state of (7) imitates the final state of (1) (see Ref. [4]).

1. One photon fulfils detection conditions i.e. $x \geqslant x_{D'}$, $-y_D \leqslant y \leqslant y_D$ where $x_D = 2E_D/\sqrt{s}$ and $y_D = \cos\theta_D$ with E_D and θ_D being the minimum photon energy to be detected and the photon tagging angle. The other photon is collinear with the initial beam, i.e. $|y_2| \leqslant y_v$ with y_v being the cosine of photon veto angle, and it is assumed to be hard that means $x_2 \geqslant x_m = 2E_m/\sqrt{s}$, where E_m is the cut energy of soft photons. In this region we cannot neglect the electron mass, because the terms $\sim m_e^2/(p_i \cdot k_i)^2$ become of the same order of magnitude as the terms $\sim 1/(p_i \cdot k_i)$ $(i = 1, 2)$ when $\vec{k}_2$ is parallel to $\vec{p}_1$ or $\vec{p}_2$. The effect of the nonzero electron mass is taken into account according to the prescription given in Ref. [15].

2. One photon fulfils the detection criteria as in 1 while the other, although satisfying $|y_2| \leqslant y_v$ and being hard, has the energy below the detection threshold i.e. $x_m \leqslant x_2 \leqslant x_v = 2E_v/\sqrt{s}$, where E_v is veto energy of photons.

3. Both photons are in the detection range, but they are collinear within an angle of θ_s and because of that they are detected as one photon with an energy E_1+E_2.

The effect of the hard bremsstrahlung correction is large and positive and it interferes with the effect of the virtual corrections.

4. Numerical results

We have calculated the energy distribution of photons for the process $e^+e^- \to \bar{\nu}\nu\gamma$ for the e^+e^- CM system energy $\sqrt{s} = 100$ GeV. The relevant input parameters are $M_Z = 93$ GeV, $\alpha = 1/137.03604$ and $A = \pi\alpha/\sqrt{2}G_\mu = (37.281\ \text{GeV})^2$. Since the W boson mass is not supposed to be known with high accuracy even at LEP II we eliminate it by means of the relation (see e.g. [16])

$$M_W^2\left(1-\frac{M_W^2}{M_Z^2}\right) = \frac{A}{1-\Delta r}, \tag{10}$$

where $\Delta r = 0.0713 \pm 0.0013$ (see Ref. [17]) is a higher order correction mainly due to γ, W and Z self energy diagrams. The result depends on the Higgs mass and fermion masses (which we set to be the same as in Ref. [18] with the exception of the t quark mass that we set to 45 GeV) through electroweak one loop corrected Z self energy and the $Z\gamma$ mixing as well as the Δr of equation (10), but this dependence is rather moderate.

We have assumed the following experimental set up

1. veto angle of $\theta_v = 5°$,
2. tagging angle of $\theta_D = 20°$,
3. minimum photon energy to be detected of $E_D = 1$ GeV,
4. two photons separation angle of $\theta_s = 1°$.

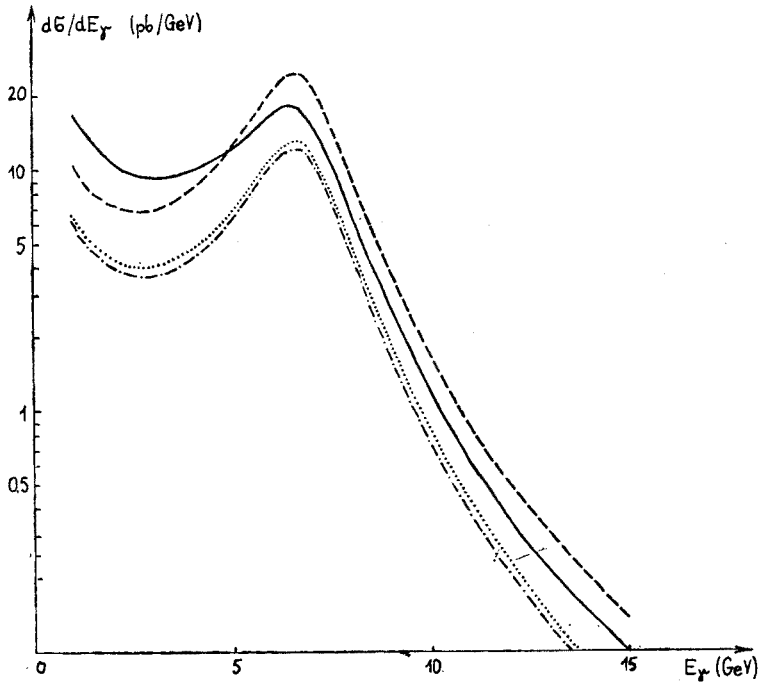

Fig. 6. Photon energy distributions for the process $e^+e^- \to \bar{\nu}\nu\gamma$ as referred to in the text

The choice of the relevant initial parameters and of the experimental cuts is similar to the one by Berends et al. [4] which makes it easier to compare both results for photon energy distribution. However, it should be stressed that we have not made the replacement (5) for the hard bremsstrahlung part as it was done in [4]. Since the analytical formula for the one loop corrected Z self energy $\Sigma_Z(Q^2)$ is rather complicated (see [9]), to save the computational time, we have calculated the hard bremsstrahlung correction with the tree-level Z propagator with $\Gamma_Z = -\mathrm{Im}\,\Sigma_Z(M_Z^2)/M_Z = 2.61$ GeV ($m_t = 45$ GeV). In Fig. 6 we have depicted the results of our calculations for the photon energy distribution $d\sigma/dE_\gamma$. The dashed line represents the Born approximation. The dashed and dotted line corresponds to the distribution with one loop QED and soft photon corrections. The dotted line represents the distribution which, apart from the virtual photonic and soft corrections, includes the weak corrections considered. The solid line corresponds to the totally corrected cross-section which, apart from the latter, also includes the hard bremsstrahlung corrections. It can be seen that the radiative corrections result in the decrement of the peak connected with the Z resonance. They also shift the peak a bit towards lower photon energies which is caused by the hard bremsstrahlung corrections. The shape of our corrected distribution (solid line) is identical with the shape of the corresponding histogram in [4], however, our distribution is shifted a bit upwards due to the additional weak corrections included.

The Born cross section integrated over the region $E_\gamma = 6.5 \pm 2.5$ GeV is of 71 pb. The photonic corrections diminish it by 50%. The weak corrections increase it by 4%. The hard bremsstrahlung corrections are positive. Region 1 contributes 24%, region 2 gives additional 4% while the contribution of region 3 is negligible. The total radiative corrections diminish the Born cross section in the photon energy region considered by 18%.

APPENDIX

In this appendix we present the analytical formula for the $m^{\mu\nu}$ of formula (8). It includes 21 traces along the electron lines of the 6 Feynman diagrams of the process (7) which occur in the average over polarizations of the initial electrons. These 21 traces can be expressed in terms of the 9 quantities $m_{ij}^{\mu\nu}$ that are given by

$$m_{11}^{\mu\nu} = -\frac{4}{(s_1^2)^2(s_{12}^2)^2}\,\mathrm{Tr}\,(\hat{p}_2\hat{s}_1\hat{s}_{12}\gamma^\mu\hat{p}_1\gamma^\nu\hat{s}_{12}\hat{s}_1),$$

$$m_{12}^{\mu\nu} = \frac{8(s_1s_2)}{s_1^2s_2^2(s_{12}^2)^2}\,\mathrm{Tr}\,(\hat{p}_2\hat{s}_{12}\gamma^\mu\hat{p}_1\gamma^\nu\hat{s}_{12}),$$

$$m_{13}^{\mu\nu} = \frac{8(r_1s_1)}{s_1^2r_1^2s_{12}^2r_{12}^2}\,\mathrm{Tr}\,(\hat{p}_2\hat{p}_1\gamma^\mu\hat{s}_{12}\hat{r}_{12}\gamma^\nu),$$

$$m_{14}^{\mu\nu} = -\frac{4}{s_1^2r_2^2s_{12}^2r_{12}^2}\,\mathrm{Tr}\,(\hat{p}_2\gamma^\nu\hat{r}_{12}\hat{s}_1\hat{p}_1\gamma^\mu\hat{s}_{12}\hat{r}_2),$$

$$m_{15}^{\mu\nu} = -\frac{4}{(s_1^2)^2 r_2^2 s_{12}^2}\,\mathrm{Tr}\,(\hat{p}_2\hat{s}_1\hat{p}_1\gamma^\mu\hat{s}_{12}\hat{r}_2\gamma^\nu\hat{s}_1),$$

$$m_{16}^{\mu\nu} = \frac{2}{s_1^2 s_2^2 r_1^2 s_{12}^2}\,\mathrm{Tr}\,(\hat{p}_2\hat{p}_1\gamma^\mu\hat{s}_{12}\gamma^\varrho\hat{s}_1\hat{r}_1\gamma^\nu\hat{s}_2\gamma_\varrho),$$

$$m_{35}^{\mu\nu} = \frac{2}{r_1^2 r_{12}^2 s_1^2 r_2^2}\,\mathrm{Tr}\,(\hat{p}_2\gamma^\mu\hat{r}_{12}\hat{p}_1\gamma^\varrho\hat{r}_1\hat{r}_2\gamma^\nu\hat{s}_1\gamma_\varrho),$$

$$m_{55}^{\mu\nu} = -\frac{4}{(s_1^2)^2(r_2^2)^2}\,\mathrm{Tr}\,(\hat{p}_2\hat{s}_1\gamma^\mu\hat{r}_2\hat{p}_1\hat{r}_2\gamma^\nu\hat{s}_1),$$

$$m_{56}^{\mu\nu} = \frac{8(p_1p_2)}{s_1^2 s_2^2 r_1^2 r_2^2}\,\mathrm{Tr}\,(\hat{r}_2\gamma^\mu\hat{s}_1\hat{r}_1\gamma^\nu\hat{s}_2),$$

where

$$\begin{aligned} r_1 &= p_1 - k_1, & s_1 &= p_2 - k_1,\\ r_2 &= p_1 - k_2, & s_2 &= p - k_2,\\ r_{12} &= p_1 - k_1 - k_2, & s_{12} &= p_2 - k_1 - k_2. \end{aligned}$$

The quantities $m_{ij}^{\mu\nu}$ can be expressed (with the use of REDUCE) by 6 invariants: $p_1 \cdot p_2$, $p_1 \cdot k_1$, $p_1 \cdot k_2$, $p_2 \cdot k_1$, $p_2 \cdot k_2$, and $k_1 \cdot k_2$ which, in the frame described below formula (8), read

$$p_1 \cdot p_2 = \frac{s}{2}, \qquad p_1 \cdot k_1 = \frac{s}{4}x_1(1-\beta y_1),$$

$$p_1 \cdot k_2 = \frac{s}{4}x_2(1-\beta y_2), \qquad p_2 \cdot k_1 = \frac{s}{4}x_1(1+\beta y_1),$$

$$p_2 \cdot k_2 = \frac{s}{4}x_2(1+\beta y_2), \qquad k_1 \cdot k_2 = \frac{s}{4}x_1x_2(1-y).$$

where notation is the same as in Section 3.

The $m^{\mu\nu}$ is given by

$$\begin{aligned} m^{\mu\nu} = [&m_{11} + m_{11}(k_1 \leftrightarrow k_2) + m_{11}(p_1 \leftrightarrow p_2)\\ &+ m_{11}(k_1 \leftrightarrow k_2,\, p_1 \leftrightarrow p_2) + m_{55} + m_{55}(k_1 \leftrightarrow k_2)\\ &+ 2(m_{12} + m_{13} + m_{14} + m_{15} + m_{16} + m_{14}(k_1 \leftrightarrow k_2)\\ &+ m_{13}(k_1 \leftrightarrow k_2) + m_{15}(k_1 \leftrightarrow k_2) + m_{16}(k_1 \leftrightarrow k_2)\\ &+ m_{12}(p_1 \leftrightarrow p_2) + m_{35} + m_{15}(p_1 \leftrightarrow p_2) + m_{56}\\ &+ m_{15}(k_1 \leftrightarrow k_2,\, p_1 \leftrightarrow p_2) + m_{35}(k_1 \leftrightarrow k_2)]^{\mu\nu}. \end{aligned}$$

REFERENCES

[1] A. D. Dolgov, L. B. Okun, V. I. Zakharov, *Nucl. Phys.* **B41**, 197 (1972).

[2] E. Ma, J. Okada, *Phys. Rev. Lett.* **41**, 287 (1978); K. J. F. Gaemers, R. Gastmans, F. M. Renard, *Phys. Rev.* **D19**, 1605 (1979).

[3] G. Barbiellini, B. Richter, J. L. Siegrist, *Phys. Lett.* **106B**, 414 (1981).

[4] F. A. Berends, G. J. H. Burgers, C. Mana, M. Martinez, W. L. van Neerven, CERN preprint TH.4865/87, Sept. 1987.

[5] M. Igarashi, N. Nakazawa, *Nucl. Phys.* **B288**, 301 (1987).

[6] M. Böhm, T. Sack, *Z. Phys.* **C35**, 119 (1987).

[7] M. Caffo, R. Gatto, E. Remiddi, *Phys. Lett.* **173B**, 91 (1986); *Nucl. Phys.* **B286**, 293 (1987); C. Mana, M. Martinez, *Nucl. Phys.* **B287**, 601 (1987).

[8] D. Karlen, *Nucl. Phys.* **B287**, 601 (1987); M. Martinez, R. Miquel, University of Barcelona preprint UAB-LFAE 87-01.

[9] K. Aoki, Z. Hioki, R. Kawabe, M. Konuma, T. Muta, *Prog. Theor. Phys.* Suppl. **73**, 1 (1981).

[10] G. Passarino, M. Veltman, *Nucl. Phys.* **B160**, 151 (1980).

[11] A. C. Hearn, REDUCE 2 user's manual, UCP-19, Univ. of Utah 1973.

[12] G. 't Hooft, M. Veltman, *Nucl. Phys.* **B153**, 365 (1975).

[13] K. Kołodziej, Ph. D. thesis submitted to the University of Silesia, Katowice 1988.

[14] B. Lautrup, RIWIAD, CERN-DD D114.

[15] F. A. Berends, R. Kleiss, P. de Causmaecker, R. Gastmans, W. Troost, T. T. Wu, *Nucl. Phys.* **B206**, 61 (1982).

[16] G. Altarelli et al., Physics at LEP, CERN 86-02.

[17] F. Jegerlehner, *Z. Phys.* **C32**, 195, 425 (1986).

[18] M. Böhm, W. Hollik, H. Spiesberger, *Fortschr. Phys.* **43**, 687 (1987).